NASA TECHNICAL NOTE

QUASI-ONE-DIMENSIONAL COMPRESSIBLE FLOW ACROSS FACE SEALS AND NARROW SLOTS

I — Analysis

by John Zuk, Lawrence P. Ludwig,
and Robert L. Johnson

Lewis Research Center
Cleveland, Ohio 44135

NATIONAL AERONAUTICS AND SPACE ADMINISTRATION • WASHINGTON, D. C. • MAY 1972

1. Report No. NASA TN D-6668	2. Government Accession No.	3. Recipient's Catalog No.
4. Title and Subtitle QUASI-ONE-DIMENSIONAL COMPRESSIBLE FLOW ACROSS FACE SEALS AND NARROW SLOTS I - ANALYSIS		5. Report Date May 1972
		6. Performing Organization Code
7. Author(s) John Zuk, Lawrence P. Ludwig, and Robert L. Johnson		8. Performing Organization Report No. E-6819
		10. Work Unit No. 132-15
9. Performing Organization Name and Address Lewis Research Center National Aeronautics and Space Administration Cleveland, Ohio 44135		11. Contract or Grant No.
		13. Type of Report and Period Covered Technical Note
12. Sponsoring Agency Name and Address National Aeronautics and Space Administration Washington, D.C. 20546		14. Sponsoring Agency Code

15. Supplementary Notes

16. Abstract

An analysis is presented for compressible fluid flow across shaft face seals and narrow slots. The analysis includes fluid inertia, viscous friction, and entrance losses. Subsonic and choked flow conditions can be predicted and analyzed. The model is valid for both laminar and turbulent flows. Results agree with experiment and with solutions which are more limited in applicability. Results show that a parallel film can have a positive film stiffness under choked flow conditions.

17. Key Words (Suggested by Author(s)) Lubrication; Subsonic flow; Choked flow; Laminar flow; Turbulent flow; Seal; Face seal; Sealing dam; Gas bearings	18. Distribution Statement Unclassified - unlimited

19. Security Classif. (of this report) Unclassified	20. Security Classif. (of this page) Unclassified	21. No. of Pages 38	22. Price* $3.00

QUASI-ONE-DIMENSIONAL COMPRESSIBLE FLOW

ACROSS FACE SEALS AND NARROW SLOTS

I - ANALYSIS

by John Zuk, Lawrence P. Ludwig, and Robert L. Johnson

Lewis Research Center

SUMMARY

An analysis is presented for compressible fluid flow across gas film shaft face seals and narrow slots. The flow is analyzed using a quasi-one-dimensional integral method which includes fluid inertia, viscous friction, and entrance losses. Viscous friction is accounted for by a mean friction factor. The model is valid for both laminar and turbulent flow. Subsonic and choked flow conditions can be analyzed.

A seal radial width to film thickness geometric parameter is used. For large values of this parameter and for low Mach number, the results are identical to the solution for viscous subsonic flow; for small values, the results correspond to orifice flow equations. Results agree with radial flow experiments.

Results show that a parallel film can have a positive film stiffness under choked flow conditions.

INTRODUCTION

Shaft seal systems in advanced aircraft turbine engines will be operated at speeds, temperatures, and pressures higher than shaft seals currently used. Conventional face seals presently used in gas turbine engines are limited to sliding velocities of about 110 meters per second (350 ft/sec), pressures of about 86 newtons per square centimeter (125 lb/in.^{2}), and gas temperatures of 700 K (800$^{\rm o}$ F) (ref. 1). Advanced engines, however, will require seals to operate to speeds of 150 meters per second (500 ft/sec) (ref. 2), pressures to 340 newtons per square centimeter (500 lb/in.^{2}), and temperatures to 980 K (1300$^{\rm o}$ F) (ref. 3). For face seals operating at these conditions, a positive face separation (no rubbing contact) will be required to achieve long life and reliability. A promising approach is the use of gas film seals with self-acting lift pads (see

Figure 1. – Pressure-balanced face seal with self-acting lift pads (added for axial film stiffness).

fig. 1, refs. 4 and 5, and Seal Description and Models).

Since the seals must be pressure balanced, a proper balance of the opening and closing forces must be achieved with a leakage gap that has tolerable mass leakage. The gap must be small enough so that the leakage is minimal, but it must be large enough so that power dissipation, due to shear in the film, and face deformation are tolerable. Thus the design of the sealing gap is vital to seal performance and pressure distribution in the gap and mass leakage through the gap must be analyzed. In this report only the sealing dam portion of the seal is analyzed.

The classical viscous, isothermal, subsonic, compressible flow analysis for this problem is well known (e.g., see Gross, ref. 6). The pressure distribution and mass leakage have been calculated for the parallel film hydrostatic case. Carothers (ref. 7) has conducted compressible flow experiments in thin films of air which are flowing radially between parallel plates. The pressure distribution was found for both subsonic and supersonic axial entrance flows. Carothers' geometry, however, was representative of externally pressurized gas bearings rather than seals. Grinell (ref. 8) has theoretically and experimentally investigated compressible flow in thin passages and has shown agreement between theory and experiment. Mueller (ref. 9) included compressibility for the case where there was a restricted bypass orifice flow into the parallel gap, but his analysis did not consider conditions which would yield choked flow in the

gap. The textbook on mechanical face seals by Mayer (ref. 10) virtually excluded face seal operation under conditions where fluid compressibility is important.

The objective of this report is to present a mathematical analysis of compressible fluid flow across shaft face seals and narrow slots. The analysis includes fluid inertia, viscous friction, and entrance losses and thus describes both subsonic and choked flow conditions. For specified pressure ratios, film thicknesses, and friction factor variations with Reynolds number, which are used as parametric input, the output variables include mass and volume leakage flow rates, force, center of pressure, and distributions of pressure, density, velocity, temperature, and Mach number.

Seal Description and Models

A conventional face seal which is pressure (force) balanced is shown in figure 2. In this seal, the pressure drop occurs across a narrowly spaced sealing dam, and the force due to this pressure drop is balanced by a hydrostatic closing force and spring force. This configuration, however, has an inherent problem. For parallel sealing dam surfaces, the force caused by the pressure drop across the sealing dam is independent of film thickness for low Mach numbers; hence, there is no way of maintaining preselected film thickness which will allow tolerable leakage and still have noncontact operation. Since the force is independent of film thickness, the design also lacks axial film stiffness for sufficient dynamic tracking of the stationary nosepiece with the rotating seal seat. In order to operate adequately, the seal nosepiece must follow the seal seat surface under all conditions without surface contact or excessive increase in film
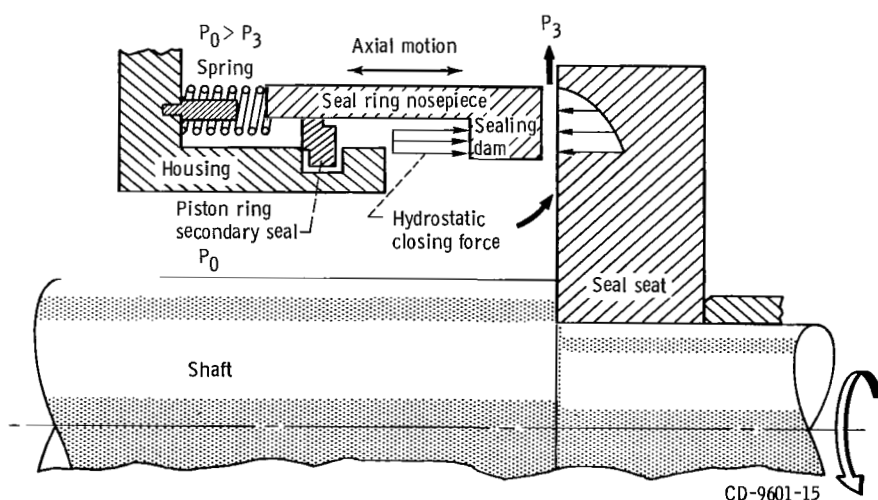

Figure 2. - Pressure-balanced face seal with no axial film stiffness.

thickness, which would yield high leakage. Some of these conditions are axial runout, misalinement, thermal distortion, coning, and dishing.

A promising method of maintaining a preselected film thickness and achieving axial film stiffness is to add a self-acting gas bearing, such as shrouded Rayleigh step lift pads, to the conventional rubbing contact pressure-balanced face seal (see fig. 1 for a sketch and refs. 4 and 5 for details of this concept, design, and test results). Both the sealing dam force due to the pressure drop across the sealing dam and the self-acting lift pad (gas bearing) force are balanced by the hydrostatic and spring closing forces. The gas bearing has a desirable characteristic whereby the force increases with decreasing film thickness. If the seal is perturbed in such a way as to decrease the gap, the additional force generated by the gas bearing will open the gap to the original equilibrium position. In a similar manner, if the gap becomes larger, the gas bearing force decreases, and the closing force will cause the seal gap to return to the equilibrium position.

Some Models and Their Limitations

For subsonic flow, variable cross-sectional area, and Mach number $< 1/\sqrt{\gamma}$ (all symbols are defined in appendix A), the analysis of reference 11 can be used. This differential analysis finds a solution for the case where the viscous friction is balanced by the pressure drop and the fluid inertia is negligible. For this condition the entrance pressure drop is small; hence, $P_0 = P_1$ and $P_2 = P_3$ (see fig. 3). The flow is nearly isothermal for the film thickness range studied. The analysis of reference 11 yields the classical cubic dependence of mass flow on film thickness. Also, this analysis enables
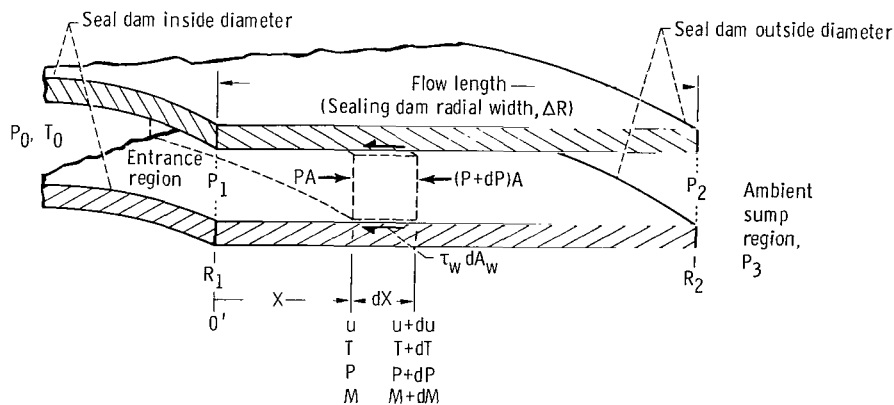

Figure 3. - Model and notation of sealing faces including control volume for quasi-one-dimensional flow.

small tilts of the sealing dam surfaces to be studied. These small tilts simulate seal face deformations which can occur due to thermal, centrifugal, etc., effects.

For flow approaching Mach 1 (i.e., choked flow), the inertia force neglected in reference 11 becomes important. Also, the flow behaves more as an adiabatic flow than an isothermal flow. The equations (partial differential equations) are relatively complex because of the nonlinearity of the inertia terms; thus an approximate analytical model must be used. In the approximate model presented here, the flow is analyzed as a quasi-one-dimensional flow using a control volume integral analysis.

Since in gas film face seal applications there is seal seat rotation relative to the seal nosepiece, a question arises as to the validity of neglecting the centripetal inertia force which would affect the radial flow. This question was examined in reference 13. It was found that the circumferential rotational flow can be uncoupled from the radial pressure flow when the ratio of rotational velocity to pressure flow velocity is less than $1/\sqrt{Re(h/\Delta R)}$. Rotational effects are important for calculating the viscous shear and power dissipation.

It should be pointed out that the flow in a gas film face seal is qualitatively quite different from the flow in an externally pressurized thrust bearing. Both operate with very small film thicknesses, usually less than 0.0025 centimeter (1 mil). However, gas film face seals are characterized by a small $(R_2 - R_1)/R_1$ ratio. Also, the inner cavity is a large supply reservoir. Hence, in gas film seals the reservoir pressure does not vary with film thickness. On the other hand, externally pressurized gas thrust bearings are characterized by a large $(R_2 - R_1)/R_1$ ratio. (The large surface area is necessary for high load capacity.) In order to maintain positive film stiffness, compensating inlet flow restrictors are used. Because of these restrictors, the inlet pressure to the bearing varies significantly with film thickness. As a result of these differences, the flow regimes for the two cases are quite different.

QUASI-ONE-DIMENSIONAL FLOW ANALYSIS

As stated in the previous section, when the radial flow is close to choked or is choked at the exit, the viscous flow analysis in reference 11 is no longer valid. Fluid inertia, neglected in that analysis, becomes important. The rigorous inclusion of inertial terms necessitates the solution of nonlinear partial differential equations and is therefore not practical for engineering calculations; hence an approximate analytical model will be formulated which will be especially useful for calculating flow conditions near and at choking.

The geometry is shown in figure 3. Two parallel, coaxial, circular rings are separated by a very narrow gap. Rotational effects on the radial flow are negligible for

most applications (ref. 13). A pressure differential exists between the rings' inner and outer radii. The cavities on either side (i.d. and o.d.) of the sealing dam are assumed to be constant pressure reservoirs. For subsonic flow, reservoir conditions and the exit ambient pressure are specified. For choked flow, reservoir conditions and an exit Mach number of one are specified.

The analysis can be separated into two parts, which can then be considered separately. One part is an analysis of the seal passage itself, in which the flow is assumed to behave as a constant area, adiabatic flow with friction, while the other part is an analysis of the entrance flow. The analysis for these two regions is described first followed by a discussion of the iterative procedure for the complete solution.

Constant Area Adiabatic Flow With Friction

It is assumed that the flow in the seal leakage flow region behaves as a constant area adiabatic flow with friction. A quasi-one-dimensional approximation is made wherein it is assumed that the flow properties can be described in terms of their cross-sectional averages.

The following assumptions have been made in the analysis:

(1) The area expansion due to radius increase is neglected. (In most mainshaft face seals the i.d./o.d. is about 0.98.)

(2) The flow is adiabatic.

(3) No shaft work is done on or by the system.

(4) No potential energy differences are present such as caused by elevation differences.

(5) The fluid behaves as a perfect gas.

(6) The sealing surfaces are parallel.

With these assumptions, the flow is commonly known as Fanno line flow (ref. 15). This analysis is similar to that used by Grinnell (ref. 8) for flow in thin passages. The governing equations when area changes are neglected are as follows:

Conservation of mass:

$$\dot{M} = \rho u A = \text{constant} \tag{1}$$

which reduces to

$$\frac{d\rho}{\rho} + \frac{1}{2}\frac{du^2}{u^2} = 0 \tag{2}$$

6

Conservation of energy:

$$e + \frac{P}{\rho} + \frac{u^2}{2} = \text{constant}$$

or

$$i + \frac{u^2}{2} = \text{constant} \tag{3}$$

where i is the specific enthalpy. This can be written as

$$di = c_p \, dT = -\frac{1}{2} \, du^2 \tag{4}$$

This equation can be reduced to

$$\frac{dT}{T} + \frac{(\gamma - 1)}{2} M^2 \frac{du^2}{u^2} = 0 \tag{5}$$

where the Mach number $M = u/\sqrt{\gamma \Re T}$.

Equation of state:

$$P = \rho \Re T \tag{6}$$

or

$$\frac{dP}{P} = \frac{d\rho}{\rho} + \frac{dT}{T} \tag{7}$$

Conservation of momentum:

$$- A \, dP - \tau_w \, dA_w = M \, du \tag{8}$$

Now the hydraulic diameter and Fanning friction factor are introduced:

$$D = \frac{4A}{\dfrac{dA_w}{dX}}$$

$$f = \frac{\tau_w}{\dfrac{\rho u^2}{2}}$$

It is assumed that the viscous effect can be represented by a mean friction factor. The mean friction factor depends on Reynolds number only and is a slowly varying function of Reynolds number for many flows, geometries, and conditions.

The set of equations ((2), (5), (7), and (8)) can be combined into a single equation in terms of the Mach number alone. Details of obtaining this equation can be found in appendix B. The result is

$$\frac{4f}{D} dX = \frac{(1 - M^2)\, dM^2}{\gamma M^4 \left(1 + \dfrac{\gamma - 1}{2} M^2\right)} \tag{9}$$

This equation can now be integrated from some location X_a (where the Mach number is M_a) to the location X_b (where the Mach number is M_b). By the use of partial fractions, the right side of equation (9) can be integrated to

$$\int_{M_a}^{M_b} \frac{(1 - M^2)}{\gamma M^4 \left(1 + \dfrac{\gamma - 1}{2} M^2\right)} \, dM^2 = B(M_a) - B(M_b) \tag{10}$$

where

$$B(M) = \frac{1}{\gamma} \frac{1 - M^2}{M^2} + \frac{\gamma + 1}{2\gamma} \ln \frac{\dfrac{\gamma + 1}{2} M^2}{1 + \dfrac{\gamma - 1}{2} M^2} \tag{11}$$

8

Since the variation of f with X is usually unknown, the integral of the left side of equation (9) cannot be evaluated exactly. However, if f is replaced by an appropriate mean value $\bar{f}$, the integration may be performed:

$$\frac{4}{D} \int_{X_a}^{X_b} f\, dX = \frac{4\bar{f}}{D} (X_b - X_a) \tag{12}$$

The integration of equation (9) yields

$$\frac{4\bar{f}}{D} (X_b - X_a) = B(M_a) - B(M_b) \tag{13}$$

In the computer calculation, it is convenient to define a length

$$L_N = X_{max} - X_N \tag{14}$$

such that

$$\frac{4\bar{f}}{D} (X_{max} - X_N) = \frac{4\bar{f}\, L_N}{D} \tag{15}$$

$$\frac{4\bar{f}\, L_N}{D} = B(M_N) \tag{16}$$

(Note that $B(M = 1) = 0$.) The length L_N is the length of the seal (measured from X_N) for which the condition at the exit is sonic (choked). It follows, if M_1 and M_2 are the Mach numbers at the inlet and exit of the seal, respectively, that

$$\Delta R = L_1 - L_2 \tag{17}$$

See figure 4.

The reservoir pressure and exit ambient static pressure are known. It is desirable to find the pressure at any point in the flow leakage passage as a function of Mach num-
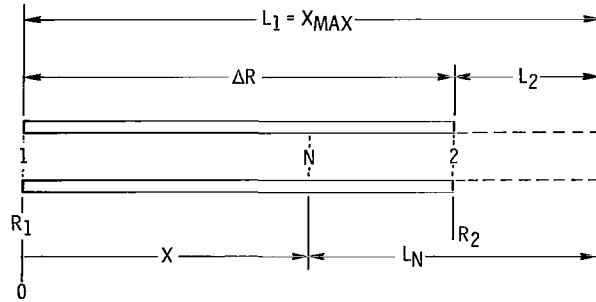
Figure 4. - Lengths and stations used in the analysis. (Subsonic case is shown.)

ber. The flow is adiabatic. Thus the stagnation temperature is constant everywhere in the seal; that is,

$$T_{01} = T_{02} \tag{18}$$

or (ref. 15, p. 80)

$$T_1 \left(1 + \frac{\gamma - 1}{2} M_1^2\right) = T_2 \left(1 + \frac{\gamma - 1}{2} M_2^2\right) \tag{19}$$

From this relation, the continuity equation, the equation of state, and the definition of the Mach numbers, one obtains

$$\frac{P_1}{P_2} = \frac{M_2}{M_1} \sqrt{\frac{1 + \frac{\gamma - 1}{2} M_2^2}{1 + \frac{\gamma - 1}{2} M_1^2}} \tag{20}$$

Entrance Flow

If it is assumed that the flow in the entrance region is isentropic and adiabatic, the analysis is straightforward. The adiabatic energy equation is

$$i_0 = i_1 + \frac{u_1^2}{2} \tag{21}$$

which can be written as

$$\frac{T_0}{T_1} = 1 + \frac{(\gamma - 1)M_1^2}{2} \tag{22}$$

By use of the isentropic relation, $P/\rho^\gamma = $ constant, and the equation of state, other inlet variables can be found knowing the sealed high pressure reservoir values; for example,

$$\frac{P_0}{P_1} = \left(\frac{T_0}{T_1}\right)^{\gamma/(\gamma-1)} = \left(1 + \frac{\gamma - 1}{2} M_1^2\right)^{\gamma/(\gamma-1)} \tag{23}$$

$$\frac{\rho_0}{\rho_1} = \left(\frac{P_0}{P_1}\right)^{1/\gamma} = \left(1 + \frac{\gamma - 1}{2} M_1^2\right)^{1/(\gamma-1)} \tag{24}$$

It is well known that entrance flows do not behave as isentropic flows but that an additional pressure drop is present due to viscous friction, turning losses, etc. A practical way of accounting for the entrance loss is to introduce an empirically determined velocity loss coefficient C_L (see appendix C). Hence, equation (22) becomes

$$T_1 = \frac{T_0}{1 + \dfrac{(\gamma - 1)M_1^2}{2C_L^2}} \tag{25}$$

while equation (23) becomes

$$P_1 = \frac{P_0}{\left[1 + \dfrac{(\gamma - 1)M_1^2}{2C_L^2}\right]^{\gamma/(\gamma-1)}} \tag{26}$$

Under the entrance conditions discussed in appendix C, the entrance velocity loss coefficient C_L is related to the head loss coefficient k' commonly used in hydraulics by the relation

$$k' = \frac{1}{C_L^2} - 1 \tag{27}$$

Iteration Procedure

The procedure for solving the previous equations is an iterative one. The solution is found using a computer program which appears in reference 12. In the iterative procedure, the first step is to solve for the minimum film thickness for which the flow is choked. If the actual film thickness is less than this minimum value, the speed of the flow is less than sonic at the exit and the exit condition is $P_2 = P_3$. If the actual film thickness is greater than the minimum for choked flow, the exit flow is sonic and the exit condition is $M_2 = 1$, but the exit pressure is unknown. The details of the procedure are as follows:

Choked film thickness evaluation. - When the flow is just choked, it is known that $P_2 = P_3$ and $M_2 = 1$. By combining equation (26), the relation for P_0/P_1, with equation (20), the equation for $P_1/P_2 = (P_1/P_3)$ in the seal leakage passage, one obtains

$$\left(\frac{P_0}{P_1}\right)\left(\frac{P_1}{P_3}\right) = \frac{P_0}{P_3} = \frac{\left(1 + \frac{\gamma - 1}{2}\right)^{1/2}}{M_1} \frac{\left[1 + \frac{\gamma - 1}{2}\left(\frac{M_1}{C_L}\right)^2\right]^{\gamma/(\gamma-1)}}{\sqrt{1 + \frac{1}{2}(\gamma - 1)M_1^2}} \tag{28}$$

Since P_0/P_3 is known, the Mach number M_1 can then be determined from this equation. Once the Mach number is known, all other flow quantities can be determined. The minimum choked film thickness is calculated as follows:

(1) A film thickness h is assumed (chosen to be 1 mil in the computer program).

(2) A Reynolds number is calculated from this film thickness.

(3) This Reynolds number determines the flow regime, laminar or turbulent, and therefore the friction factor. ($\bar{f}$ = constant/Re^n, where the constant and exponent n are program inputs and depend on whether the flow is laminar or turbulent.)

(4) A film thickness is then calculated by use of equation (16):

$$B(M_1) = \frac{4\bar{f}\,\Delta R}{D} = \frac{2\bar{f}\,\Delta R}{h} \tag{29}$$

(For radial flow between coaxial parallel disks and parallel plates, the hydraulic diameter $D = 2h$.) If this h does not agree with the previous h, steps (2) to (4) are repeated until the h's agree. This defines the critical or minimum choked film thickness h^*. It should be noted that equation (28) cannot be solved for all values of P_0/P_3, C_L, and γ. Consequently, h^* cannot be found. This condition arises for very low subsonic flows; hence, the flow is assumed to be subsonic.

Subsonic flow case. - For input film thickness less than the minimum choked film thickness, the flow is subsonic and the exit condition is $P_2 = P_3$. In this case it is convenient to use the length L_N defined by equation (14); that is, refer all quantities to a fictitious length of the seal for which the condition at the exit is sonic (choked). To start the iteration procedure, the entrance Mach number M_1 is assumed to be the same as for critical flow. All other quantities at the inlet are then calculated. The value of the friction parameter $B(M_1)$ is found from equation (11) and the choking length from equation (16); that is, $L_1 = B(M_1)D/4\bar{f}$. The length L_2 can be calculated from $L_2 = L_1 - \Delta R$ and then the friction parameter $B(M_2)$ from equation (11). Once $B(M_2)$ is known, the Mach number M_2 can be determined and, hence, the pressure P_2. This procedure is then repeated with a new Mach number M_1 until $P_2(M_1) = P_3$.

Choked flow case. - For choked flow, the input film thickness is greater than the choking film thickness and the exit condition is $M_2 = 1$. As in the subsonic flow case, the iteration procedure begins with the entrance Mach number assumed to be the choking film thickness entrance Mach number. Again all entrance quantities are calculated. The friction factor $\bar{f}$ is calculated from the Reynolds number, and the friction parameter $B(M_1) = 4\bar{f} L/D$ is calculated from equation (11). The trial flow length L is calculated as

$$L = \frac{B(M_1)D}{4\bar{f}} \tag{30}$$

If L is not equal to the true flow length ΔR, the procedure is repeated with a new M_1 until L does agree with ΔR.

Calculation of Variables at Intermediate Points

Once the entrance conditions are known, the Mach number, temperature, velocity, and pressure are determined at each desired location X_N along the seal passage length in the following way:

(1) L_N is found from equation (14).

(2) $B(M_N)$ is calculated from equation (16).

(3) M_N is found by an iterative solution of equation (11).

(4) T_N is found from equation (19) where $T_2 = T^*$ and $M_2 = 1$; hence,

$$T_N = \frac{\left(\dfrac{1 + \gamma}{2}\right) T^*}{\left(1 + \dfrac{\gamma - 1}{2} M_N^2\right)} \tag{31}$$

(5) The velocity u_N is found from the Mach number definition.

(6) The density is found from the mass conservation equation (1):

$$\rho_N = \frac{\rho_1 u_1}{u_N}$$

(7) The pressure is found from the perfect gas law, equation (6).

Computer Program

The computer program in reference 12 used to carry out this analysis is written in FORTRAN IV. The program is described in detail including all input and program variables and output options. Program listing and flow charts are presented and a sample problem with computer printout is given. The input and output can be in either the U.S. Customary or International System of Units.

Remarks on Physics of Flow

Static pressure drops to overcome flow friction. This pressure drop increases the specific volume of the fluid. Since the area change is negligible, the mean velocity must increase as the specific volume increases in order to maintain the same mass flow rate at each section of the leakage path. As the velocity increases the fluid momentum also increases, which requires an additional pressure drop. This results in a still greater increase in specific volume. This process will continue until the end of the leakage path or until the fluid reaches the maximum (choking) condition which will occur when the Mach number is one at the exit (exit velocity is sonic). Should the Mach number reach a value of one somewhere along the leakage path interior, it is expected that

14

behavior similar to duct flow will occur. For duct flow it can be shown that the flow process will adjust itself until the point at which the Mach number reaches one is shifted to the exit of the leakage passage. The mass flow rate of the fluid is the maximum which can be handled for a given inlet density and passage cross-sectional area. This flow process is known classically as Fanno line flow.

The entrance velocity head loss is negligible in subsonic viscous flow compared to the total seal pressure drop; however, under choked conditions the entrance velocity head loss is no longer negligible. This results in an entrance pressure loss. Also under choked flow conditions, the exit pressure is larger than the sump pressure and increases with film thickness. The pressure decreases through expansion waves to the sump pressure in the outer cavity. However, these expansion waves do not significantly affect the axial force balance on a seal nosepiece.

As previously stated, in most face seals the area expansion is negligible due to the radius ratios being close to one. Hence, if the flow becomes choked it will usually be at the exit. Choking can occur at the entrance under some conditions. If there is flow separation at the entrance (due, e. g., to the flow turning into the sealing faces), there could be a large entrance area decrease with choking occurring at the vena contracta. For smaller radius ratios such as those that characterize externally pressurized gas bearings, choking will occur at the entrance.

RESULTS AND DISCUSSION

The computer program from reference 12 was used to carry out the quasi-one-dimensional flow analysis. Several problems have been solved by using this program. One such problem is a case used in the design study of reference 5. The sealed pressure and temperature were 45 newtons per square centimeter absolute (65 psia) and 311 K (100° F), respectively. The exit ambient pressure was 10.3 newtons per square centimeter absolute (15 psia). The sealing dam radial width (seal leakage passage length) was 0.127 centimeter (50 mils). Figure 5 shows the calculated seal gas leakage as a function of film thickness, which ranges from 0.003 to 0.0051 centimeter (0.12 to 2 mils).

The analysis agrees with the differential analysis of reference 11, which is the classical compressible viscous analysis for subsonic viscous flow when the Mach number is less than $1/\sqrt{\gamma}$. As shown in figure 5, for film thicknesses less than 8 micrometers (0.3 mil), the Mach number is less than $1/\sqrt{\gamma} = 0.845$ and the leakage dependence on film thickness is the classical cubic dependence. The isothermal viscous flow model loses its validity when the Mach number exceeds $1/\sqrt{\gamma}$. The present approximate model, however, is valid for both subsonic and choked flow. Figure 5 shows that for
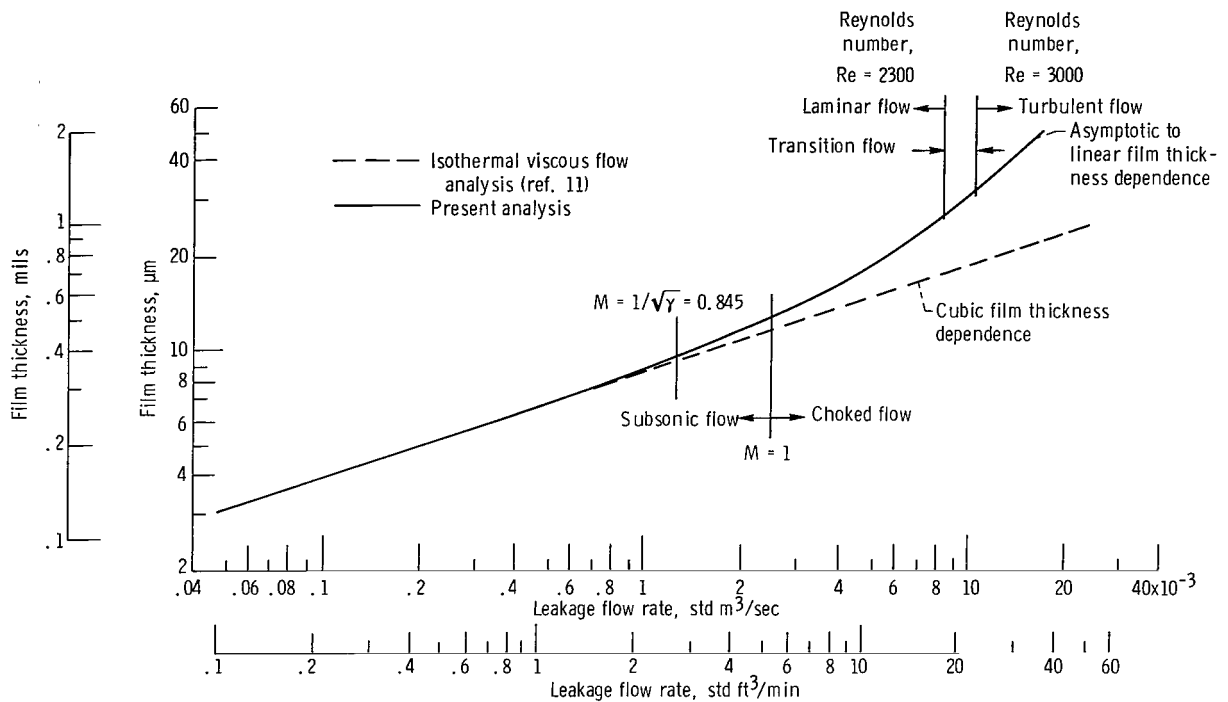
Figure 5. – Seal gas leakage as function of film thickness for parallel sealing dam surfaces. Radial dam width, ΔR, 0.130 centimeter (50 mils); sealed air pressure, P_0, 45 newtons per square centimeter absolute (65 psia); sealed air temperature, T_0, 310 K (100° F); sump pressure, P_3, 10 newtons per square centimeter absolute (15 psia).

gaps larger than 8 micrometers (0.3 mil) the leakage has a less than cubic dependence on film thickness. Note that choking occurs at a film thickness of 13 micrometers (0.52 mils). The limiting case of orifice flow, in which the flow rate varies linearly with film thickness, would be achieved when the film thickness approaches the order of the sealing dam width of 0.127 centimeter (50 mils).

As indicated in figure 5, transition from laminar to turbulent flow occurs for a film thickness of approximately 0.0033 centimeter (1.3 mils). A Reynolds number, based on hydraulic diameter, equal to 2300 has been chosen to be the critical transition Reynolds number. This appears to be a universal critical transition Reynolds number for flows in ducts, pipes, and bearings. For laminar flow, a mean Fanning friction factor of $24/Re_{2h}$ was used. This friction factor is derived from the classical, viscous compressible flow solution in reference 11 and is shown in appendix D. For turbulent flow, the Blasius friction factor - Reynolds number relation was chosen. The mean friction factor equals $0.079/Re^{1/4}$. For the transition flow regime the exact nature of the flow (hence, friction factor) is complex and not fully understood. The friction factor used for this flow regime is derived in reference 12 by assuming a smooth transition from the laminar friction factor to the turbulent friction factor. Reynolds numbers in the 2300 to 3000 range are arbitrarily selected as the transition flow regime.

16

Correlation With Experiment

Experiments were conducted at the Lewis Research Center to check the validity of the model for choked flow and for a radial geometry representative of face seals.

Leakage flow was studied for a face seal geometry (14 cm (5.50 in.) inner diameter 15.2 cm (6.00 in.) outer diameter, separated by a fixed parallel gap of 0.0038 cm (1.5 mils)). The reservoir pressure of 41.8 newtons per square centimeter absolute (60.6 psia) was held fixed while the exit pressure varied. Figure 6 shows a comparison of this analysis, the classical viscous subsonic flow differential analysis, and the radial flow experiment. Notice that the experiment shows that the flow does become choked. The maximum flow rate (choked) is 0.0080 kilogram per second (0.0176 lbm/sec). The present analysis predicts a slightly higher mass flow but agreement is within 19 percent over most of the range. On the other hand, classical compressible viscous flow theory
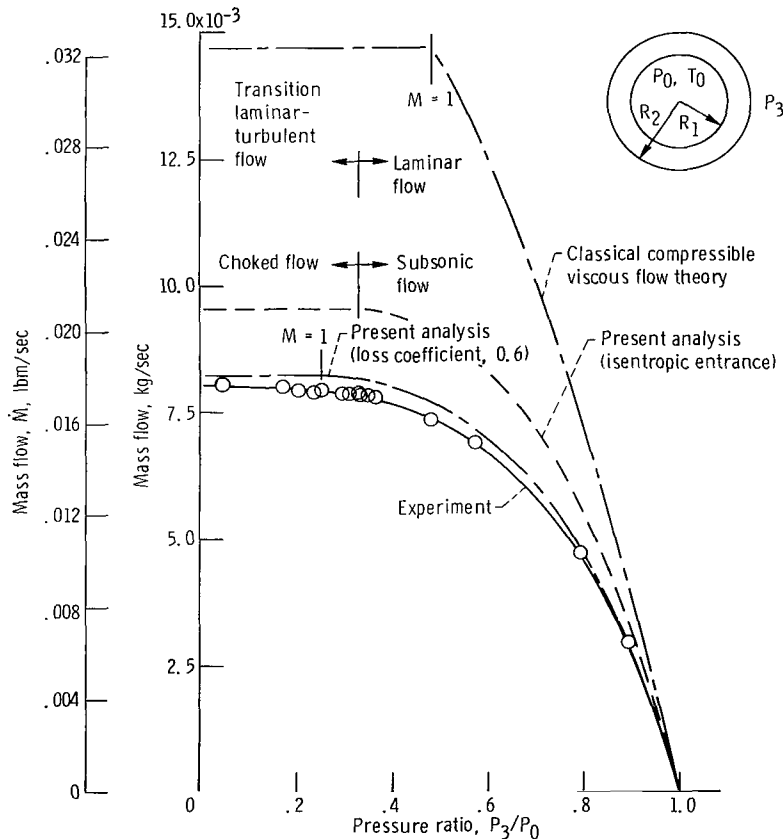
Figure 6. - Comparison of classical viscous flow theory and present analysis with radial flow experimental results. Sealed air pressure, P_0, 41.8 newtons per square centimeter (60.6 psia); sealed air temperature, T_0, 300 K (80° F); film thickness, h, 0.0038 centimeter (1.5 mils); entrance radial width, R_1, 6.98 centimeters (2.75 in.); exit radial width, R_2, 7.62 centimeters (3.00 in.); sump pressure P_3 varied.

17

overestimates the flow rate considerably at all pressure ratios except very near one. The classical theory predicts no limiting mass flow. However, if the limit is chosen as the mass flow when the Mach number is unity, predicted flows are about 80 percent higher than those observed experimentally for choked flow.

The present analysis used a friction factor of $24/Re_{2h}$ over the laminar flow region. The good agreement in figure 6 indicates that this value should be sufficient for engineering purposes. The important point is that it was derived analytically from classical compressible viscous flow theory. As is the case with duct flow, it appears to be nearly invariant with compressibility. Exact agreement could have been achieved if a different friction factor had been used. In this case almost exact agreement with the experimental curve would be achieved if $\bar{f}$ were chosen to be $6/Re^{0.76}$; however, it may not be a reliable predictor for other experiments and applications.

There are many possible reasons for the disagreement between the analytical and experimental results. It is extremely difficult to maintain a uniform film thickness for the gap sizes of interest as small as 0.0038 centimeter (1.5 mils). Problems in clamping, machining tolerances, and distortions due to large pressure differentials result in experimental error. Another possible source of disagreement between theory and experiment could be due to area expansion, which the theory neglects. In the experiment, the inner diameter to outer diameter ratio is 0.92. Thus one could expect a lower flow rate than calculated. (Calculated mass flow is based on the arithmetic mean diameter.)

The theory also assumed isentropic entrance flow conditions. For large pressure differentials the entrance velocity is large enough to cause a substantial entrance pressure drop. The result of accounting for this entrance loss condition would also result in a decrease in mass flow. As illustrated in figure 6, an entrance velocity loss coefficient equal to 0.6 gave excellent agreement with experiment.

Since the Mach number is defined using the mean flow velocity, the flow will choke locally at the centerline sooner than that predicted here at unit Mach number. The criteria used in this analysis would be accurate if a slug profile were present. Therefore, the prediction may be better for turbulent flow. Because physically there is no slip on the walls, the flow should never have an exact limit. The experimental data in figure 6 show this; however, as shown in figure 6, as the pressure ratio P_3/P_0 is decreased below 0.25, the mass flow can be considered choked for engineering purposes. Note the asymptotic behavior which shows a very small increase in mass flow with decreasing exit pressure.

The radial flow experiment was repeated for two other reservoir pressures. The experimental results are shown in figures 7 and 8 and compared with the analysis. For a reservoir (sealed) pressure of 27.6 newtons per square centimeter absolute (40 psia), the flow was laminar over the entire range studied (fig. 7). Agreement with the analysis, assuming isentropic entrance conditions, was within 18 percent. With an entrance
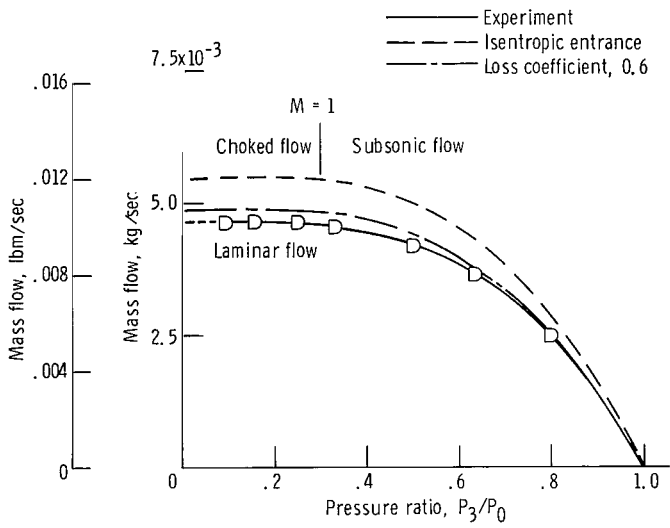
Figure 7. - Comparison of present analysis with radial flow experimental results. Sealed air pressure, P_0, 27.6 newtons per square centimeter absolute (40.0 psia); sealed air temperature, T_0, 296 K (73^0 F); film thickness, h, 0.0038 centimeter (1.5 mils); entrance radial width, R_1, 6.98 centimeters (2.75 in.); exit radial width, R_2, 7.62 centimeters (3.00 in.); laminar flow exists everywhere.
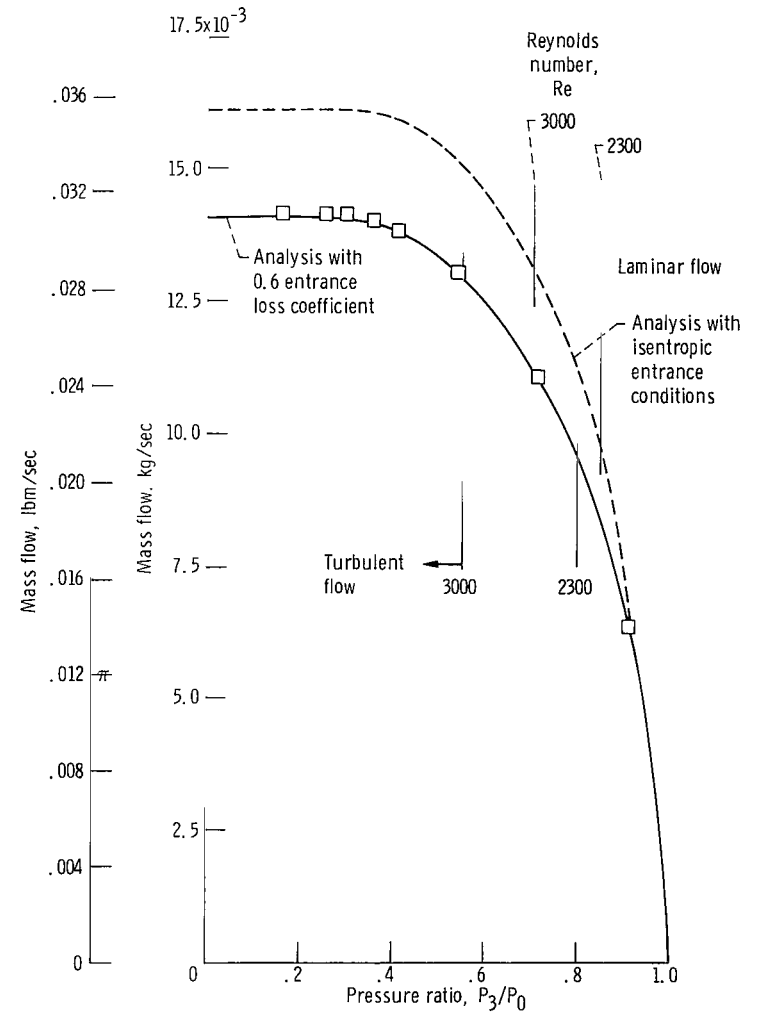

Figure 8. - Comparison of present analysis using Blasius friction factor ($\bar{f} = 0.079/Re^{1/4}$) with radial flow experimental results. Sealed air pressure, P_0, 67.1 newtons per square centimeter absolute (97.3 psia); sealed air temperature, T_0, 295 K (71^0 F); gap, 0.0039 centimeter (1.53 mils); entrance radial width, R_1, 6.98 centimeters (2.75 in.); exit radial width, R_2, 7.62 centimeters (3.00 in.).

loss coefficient of 0.6, agreement between analysis and experiment was within 5 percent.

Figure 8 shows the 67.1 newtons per square centimeter absolute (97.3 psia) reservoir pressure case experimental results compared with the analysis using the Blasius turbulent mean friction factor of $0.079/\text{Re}^{0.25}$. The inverse one-fourth dependence on Reynolds number by the friction factor occurs for many fully developed turbulent flows. The analysis with isentropic entrance conditions overestimates the flow by 13 percent; however, with an entrance loss coefficient of 0.6, there is excellent agreement with the experimental data. In the laminar flow regime the agreement is also excellent. Note the transition Reynolds number of 2300 occurred for a pressure ratio of 0.87. The turbulent flow regime was set to begin at a Reynolds number of 3000 which occurred at a pressure ratio of 0.55.

Since shaft face seals are pressure balanced, it is necessary to know the sealing dam opening force which is found from

$$F = W \int_0^{R_2 - R_1} (P - P_3)\, dX \tag{32}$$

For classical viscous, compressible flow, equation (32) is easily integrated in closed form to yield

$$F = \frac{2W(R_2 - R_1)P_1 \left[1 - \left(\dfrac{P_2}{P_1}\right)^3 \right]}{3 \left[1 - \left(\dfrac{P_2}{P_1}\right)^2 \right]} - P_3(R_2 - R_1)W \tag{33}$$

Note that the opening force is independent of the fluid properties and film thickness. This gives the well known result that parallel surfaces yield no film stiffness. However, this is not the case when the classical compressible viscous flow theory is no longer valid. Figure 9 shows a plot of seal opening force as a function of film thickness obtained using the computer program in reference 12 for both isentropic and 0.6 entrance loss cases. Notice that for small film thickness (corresponding to $M < 1/\sqrt{\gamma}$), the force is constant, as predicted by classical analysis. However, as film thickness (and Mach number) increases, the force actually increases slightly for the isentropic entrance case. This is a condition of negative film stiffness. It would be undesirable to operate in this region unless an auxiliary film stiffness generating device, such as self-acting lift pads, could make the overall seal stiffness positive. This negative stiffness
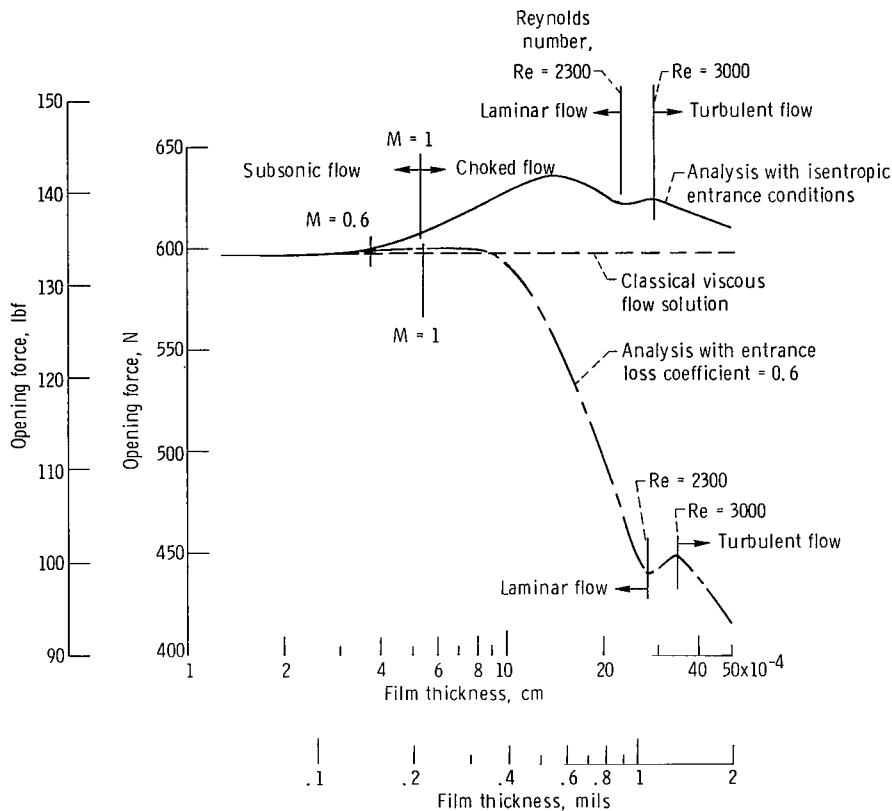
Figure 9. – Sealing dam opening force for parallel surfaces comparing classical theory with present analysis. Sealed air pressure, P_0, 148 newtons per square centimeter absolute (215 psia); sump pressure, P_3, 10.3 newtons per square centimeter absolute (15 psia); sealed air temperature, T_0, 700 K (800° F); sealing dam radial width, ΔR, 0.127 centimeter (50 mils).

may be one of the reasons why conventional gas film face seals "chatter" under certain high pressure conditions.

Also notice in figure 9 that the opening force attains a peak value and then sharply decreases with increasing film thickness. This sharp decrease indicates a high positive film stiffness which heretofore was not thought to be present for parallel surfaces.

The results using the analysis with an entrance loss coefficient of 0.6 are also shown in figure 9. The negative stiffness region has been greatly reduced; however, there is a larger region of positive film stiffness. A maximum film stiffness of about 102 000 newtons per centimeter (57 800 lbf/in.) occurs at a film thickness of 0.00152 centimeter (0.6 mil). Notice that there is another possible negative stiffness region where the flow is in transition between laminar and turbulent flow. The uncertainty of the real flow behavior in this region may mean different behavior than that calculated. Positive film stiffness also occurs in the turbulent flow regime. Of course, in an actual

seal design, the advantage gained by this added film stiffness must be weighed against the higher leakage flow resulting from choked flow operation.

Limitations of the Analysis

One of the limitations of this analysis is the neglect of the details of the flow in the entrance length. It is common in lubrication theory to neglect the entrance region entirely. This is reasonable for the slow viscous flows which characterize lubrication flows. However, when the flow becomes choked, the entrance velocities are high and it is possible that this neglect is improper.

The model developed herein may still be applied with good accuracy in cases where entrance effects are significant by using an entrance loss coefficient (see eqs. (25) to (27) and appendix C). Fleming and Sparrow have shown in reference 16 the bulk of the entrance losses occur in a small region very close to the duct inlet. Laminar incompressible entrance loss coefficients have been calculated and measured for a variety of duct shapes (e.g., refs. 16 and 17). Turbulent loss coefficients are not so widely reported; however, they may be calculated for parallel plate channels from the information in reference 18. The values for head loss coefficients k' are generally less than 20 percent of those for laminar flow. Incompressible loss coefficients may be adequate for use with compressible flow (see appendix C).

The use of the quasi-one-dimensional model can be justified by the good agreement with experiments. Also, calculations can be made very rapidly on a digital computer.

Seal Design Example

NASA has designed a seal with self-acting lift pads for potential use as a mainshaft seal in advanced gas turbine engines. This seal is described in references 4, 5, and 19. The sealing dam portion of this mainshaft face seal was designed and studied using the analysis presented herein.

Figure 10 shows the effect of sealing dam radial width on leakage flow film thicknesses from 2.5 to 0.25 micrometer (0.1 to 1 mil). The four radial dam widths used in the study were 0.051, 0.127, and 0.254 centimeter (5, 20, 50, and 100 mils). These plots illustrate that, from strictly a leakage point of view, the longest leakage path possible is most desirable. However, it is shown in reference 5 that the leakage path length must be compromised from a force balance point of view when surface deformations occur. Also shown in figure 10 is the leakage flow rate - film thickness relation for a 0.001 centimeter (0.4 mil) sealing dam radial width. Notice that at film thicknesses
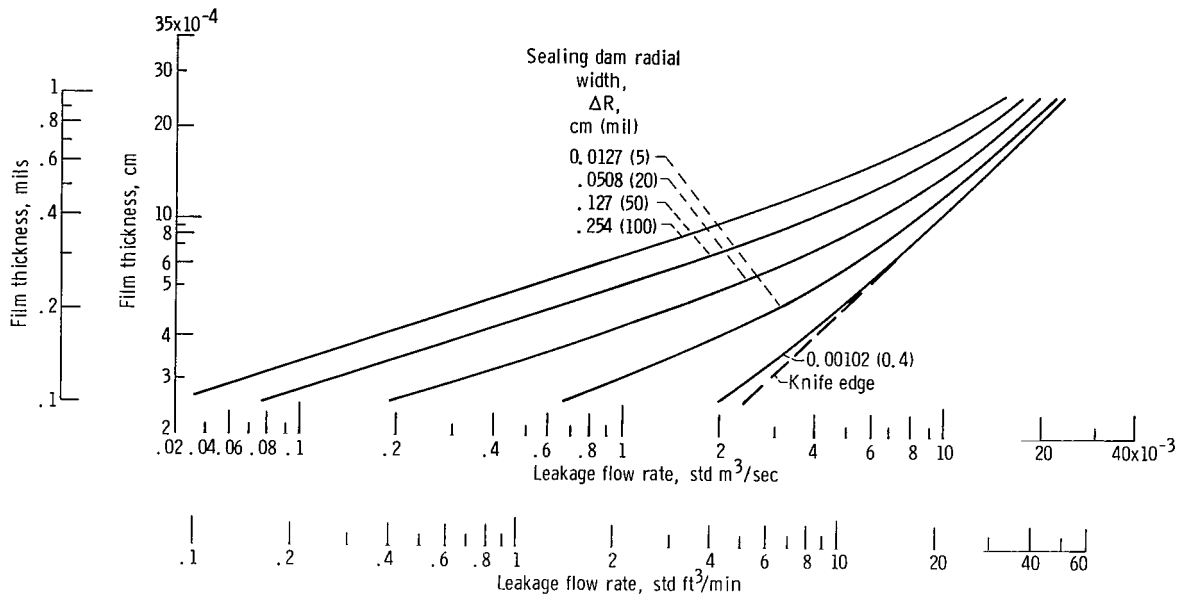
Figure 10. - Effect of seal face radial width on seal leakage. Sealed air pressure, P_0, 148 newtons per square centimeter absolute (215 psia); sump pressure, P_3, 10.3 newtons per square centimeter absolute (15 psia); sealed gas temperature, 700 K (800° F); parallel sealing faces.

greater than 0.00063 centimeter (0.25 mil) the leakage coincides with the leakage values obtained for a knife edge using the theoretical orifice flow equation. Also notice the linear variation of leakage flow with film thickness increase. For this narrow sealing dam width case when flow behaves as knife edge flow, the velocity entrance loss coefficient is the same as the flow discharge coefficient used in orifice flow analysis.

Figure 11 shows mass leakage flow as a function of pressure ratio for a fixed gap of 0.0001 centimeter (0.4 mil) and varying sealing dam width. Notice the knife edge, as expected, has the largest leakage flow rate. These values have been calculated from the theoretical orifice flow equation. The computer program result for a sealing dam width of 0.0001 centimeter (0.4 mil) agreed with the theoretical orifice flow equation. As the sealing dam width increases, the critical pressure ratio for choking decreases as indicated by the sonic line in figure 11. Again the advantage of wider (longer) sealing dams is apparent.

Recent NASA sponsored tests (ref. 19) of a shaft face seal with self-acting lift augmentation have demonstrated the feasibility of operation at gas temperatures up to 910 K (1200° F), pressure differentials across the seal up to 172 newtons per square centimeter (250 psi), and relative surface speeds up to 130 meters per second (450 ft/sec). These tests simulated the engine operating conditions such as takeoff, climb, cruise, and descent. The seal appears to be operating as predicted by the design analysis. Figure 12 shows the nosepiece seal assembly after the 120-hour endurance test. Fig-
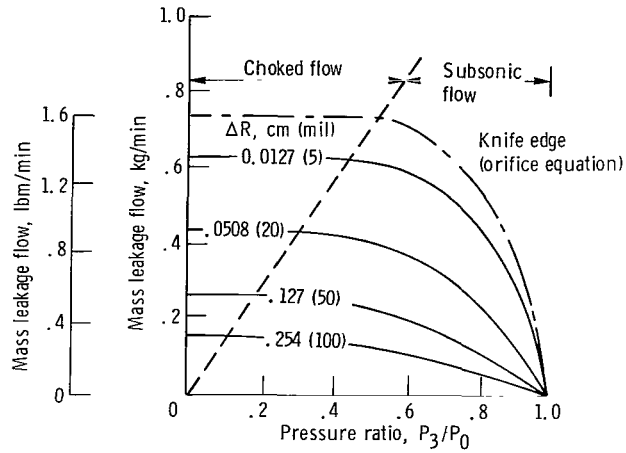
Figure 11. - Mass leakage as function of pressure ratio for various sealing dam radial widths ΔR. Sealed air pressure, P_0, 148 newtons per square centimeter absolute (215 psia); sealed gas temperature, 700 K (800° F); film thickness, h, 0.00102 centimeter (0.4 mil); entrance radial width, R_1, 8.293 centimeter (3.265 in.).
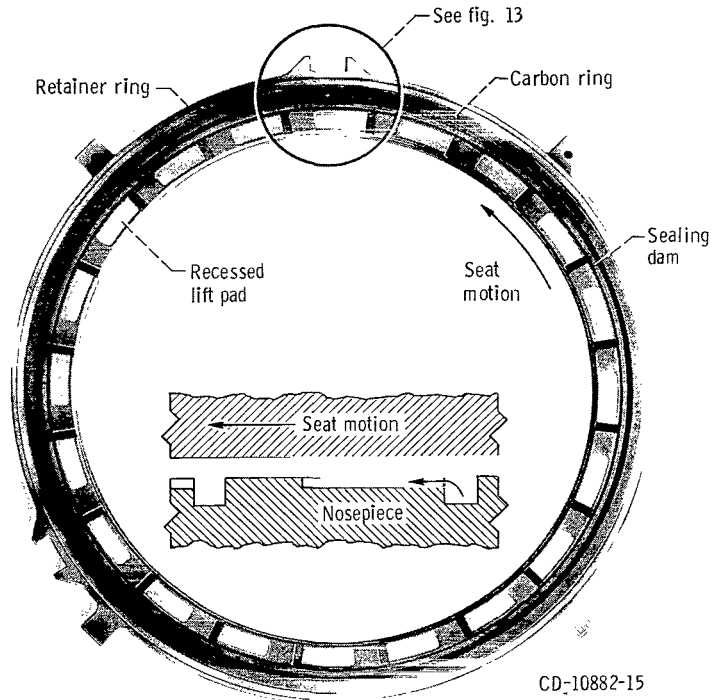

Figure 12. - Gas-film seal assembly nosepiece after 120-hour endurance test.

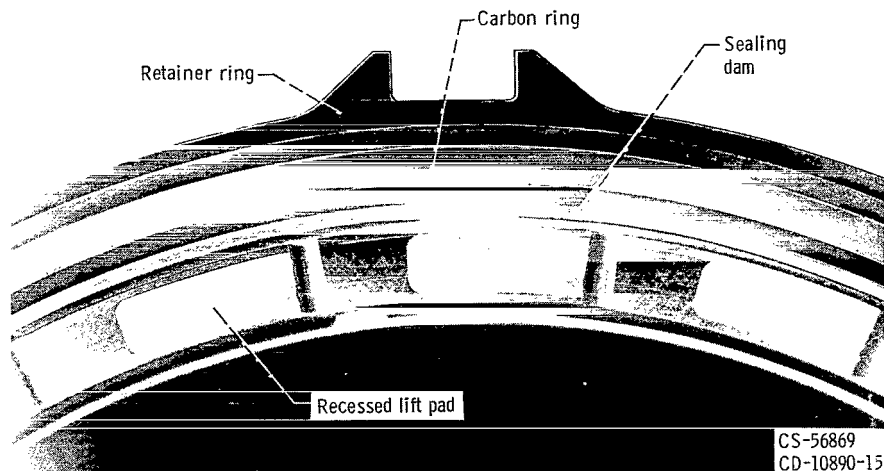Figure 13. - Closeup of carbon nosepiece of gas-film seal after 200 hours of endurance testing. Total time on seal, 338.5 hours.

ure 13 shows a closeup of the carbon nosepiece from the shaft face seal with self-acting lift pads after 320 hours of steady-state endurance testing. The total time of testing on the carbon nosepiece was 338.5 hours. The pretesting lapping marks are still observable. A surface profile trace indicated that the average wear on the surface was less than 0.13 micrometer (5 μin.). A few shallow scratches (1 to 2 μm, 50 to 100 μin.) were noticed. The test was concluded after 500 total hours of carbon nosepiece operation. The seal faces had encountered over 50 startups and shutdowns. The leakage rates varied from 5.19×10^{-3} to 15.6×10^{-3} standard cubic meter per second (11 to 32 std ft^3/min) with leakage generally averaging about 1.18×10^{-3} standard cubic meter per second (25 std ft^3/min). These leakage rates were close to those theoretically predicted.

SUMMARY OF RESULTS

An analysis has been presented for compressible fluid flow across shaft face seals. This quasi-one-dimensional integral analysis includes fluid inertia and entrance losses in addition to viscous friction which is accounted for by a mean friction factor. Subsonic and choked flow conditions can be predicted and analyzed. The model is valid for both laminar and turbulent flows. The following pertinent results were found:

1. Results agree with the classical subsonic compressible viscous flow theory for Mach numbers less than $1/\sqrt{\gamma}$. Excellent agreement with experiment is achieved if an entrance velocity loss coefficient of 0.6 is used in the laminar flow regime. The Blasius friction factor of $0.079/\text{Re}^{1/4}$ in the analysis yielded good experimental agreement in the turbulent flow regime.

2. Near and at critical flow conditions (Mach number = 1) the isentropic entrance flow analysis shows a negative film stiffness; whereas for choked flow the analysis predicts a high positive film stiffness. The analysis with an entrance loss coefficient of 0.6 predicts a high positive film stiffness for choked flow and yielded a maximum positive film stiffness of 102 000 newtons per centimeter (57 800 lbf/in.) for a design problem studied. The choked flow results contrast to classical compressible viscous flow results which show no film stiffness for parallel surfaces.

Lewis Research Center,
National Aeronautics and Space Administration,
Cleveland, Ohio, January 19, 1972,
132-15.

APPENDIX A

SYMBOLS

A   gap cross-sectional area

B   friction parameter, $\overline{4f}\ L/D$

C_L velocity entrance loss coefficient

c_P specific heat at constant pressure

D   hydraulic diameter, 2h

e   specific internal energy

F   sealing dam force

f   Fanning friction factor, $\tau_w/(\rho u^2/2)$

$\overline{f}$ mean Fanning friction factor

h   film thickness (gap)

i   specific enthalpy

k'   head loss coefficient

L_1 flow length from entrance to point of choking

M   Mach number, $u/\sqrt{\gamma \Re T}$

$\dot{M}$ mass flow

P   pressure

Q   volume leakage flow rate

r   radius

ΔR sealing dam radial width (physical flow length), $R_2 - R_1$

$\Re$ gas constant = universal gas constant/molecular weight

Re   Reynolds number, $\rho u2h/\mu$

T   temperature

u   average velocity

W   flow width

X   radial coordinate direction

z   coordinate across film thickness

μ absolute (dynamic) viscosity

γ specific heat ratio

ρ density

τ shear stress

Subscripts:

N   location along flow leakage length

w   wetted surface

0   sealed (reservoir) conditions

1   entrance conditions

2   exit conditions

3   ambient sump conditions

Superscript:

$^{-}$ average value

APPENDIX B

FRICTION FACTOR - MACH NUMBER RELATION

Equation (9) may be derived in the following way. From the equation of state (eq. (7)) and the energy equation (eq. (5)) one obtains

$$\frac{dP}{P} = \frac{d\rho}{\rho} + \frac{dT}{T} = \frac{d\rho}{\rho} - \left(\frac{\gamma - 1}{2}\right) M^2 \frac{du^2}{u^2} \tag{B1}$$

Combining this with the mass conservation equation (eq. (2)) gives

$$\frac{dP}{P} = -\frac{1 + (\gamma - 1)M^2}{2} \frac{du^2}{u^2} \tag{B2}$$

Combining equation (B2) with the momentum equation (eq. (8)) yields

$$\frac{2\gamma M^2 f}{D} dX - \left(\frac{1 - M^2}{2}\right) \frac{du^2}{u^2} = 0 \tag{B3}$$

From the definition of the Mach number ($M^2 = u^2/\gamma \Re T$) and the energy equation, one obtains

$$\left(1 + \frac{\gamma - 1}{2} M^2\right) \frac{du^2}{u^2} = \frac{dM^2}{M^2} \tag{B4}$$

Equations (B3) and (B4) then give

$$\frac{2\gamma M^2 f}{D} dX - \frac{(1 - M^2)}{2\left[1 + \frac{(\gamma - 1)}{2} M^2\right]} \frac{dM^2}{M^2} = 0 \tag{B5}$$

from which equation (9) can be obtained; that is,

$$\frac{4f}{D} \, dX = \frac{(1 - M^2) \, dM^2}{\gamma M^4 \left(1 + \frac{\gamma - 1}{2} M^2\right)} \tag{B6}$$

APPENDIX C

REMARK ON LOSS COEFFICIENT

There are several effects which cause nonisentropic pressure drops in the face seal entrance region. Because of an abrupt geometric change at the seal passage entrance, there is a nonuniform profile caused by flow turning, separated flow, and "vena contracta" effect which results in an entrance pressure drop. The pressure drop in the flow-development length is higher than that in the fully developed flow region because of two effects (ref. 16). The first effect is higher wall shear caused by higher transverse velocity gradients. The second effect is the momentum increase as the velocity distribution becomes less uniform.

The role of the entrance velocity loss coefficient may be better understood by considering the incompressible Bernoulli equation relating the stagnation reservoir pressure with the static and dynamic pressure at the seal entrance:

$$P_0 = P_1 + \frac{1}{2} \rho_1 \left(u_1 \right)^2_{\text{ideal}} \tag{C1}$$

The actual velocity at the seal entrance is less than ideal; it can be expressed as

$$u_1 = C_L \left(u_1 \right)_{\text{ideal}} \tag{C2}$$

where C_L is the entrance velocity loss coefficient (see ref. 20). Substitution of equation (C2) in (C1) and use of the Mach number definition yield

$$P_0 = P_1 + \frac{\gamma P_1 M_1^2}{2 C_L^2} \tag{C3}$$

or

$$P_1 = \frac{P_0}{1 + \dfrac{\gamma M_1^2}{2 C_L^2}} \tag{C4}$$

31

A binomial expansion of the denominator of the compressible entrance pressure equation (26) yields

$$\left[1 + \frac{1}{2}(\gamma - 1)\frac{M^2}{C_L^2}\right]^{\gamma/(\gamma-1)} = 1 + \frac{1}{2}\frac{\gamma M^2}{C_L^2} + \frac{1}{8}\frac{\gamma M^4}{C_L^4} + \frac{\gamma(2-\gamma)}{48}\frac{M^6}{C_L^6} + \cdots \qquad (C5)$$

The first two terms on the right side strongly predominate for Mach numbers less than unity. For example, when $M/C_L = 1$ and $\gamma = 1.4$,

$$\left[1 + \frac{1}{2}(\gamma - 1)\frac{M^2}{C_L^2}\right]^{\gamma/(\gamma-1)} = 1 + 0.70 + 0.18 + 0.02 + \cdots$$

The error is less than 11 percent if only the first two terms are used. The accuracy would be greater at lower Mach numbers. The first two terms of the expansion are the same as the denominator of the Bernoulli equation (C4) for a gas behaving as a quasi-incompressible fluid. Using this observation the relation between the entrance velocity loss coefficient C_L and head loss coefficient k' commonly used in hydraulics can be found. The incompressible Bernoulli equation with a head loss coefficient is

$$P_0 - k'\frac{\rho u_1^2}{2} = \frac{\rho_1 u_1^2}{2} + P_1 \qquad (C6)$$

or

$$P_1 = P_0 - (k' + 1)\frac{\rho_1 u_1^2}{2}$$

$$= P_0 - (k' + 1)\frac{\gamma P_1 M_1^2}{2} \qquad (C7)$$

Comparing equation (C7) with equation (C3) yields

$$k' = \frac{1}{C_L^2} - 1 \qquad (C8)$$

This relation enables one to convert head loss coefficients reported in the literature to velocity loss coefficients C_L, which are more convenient to use in Mach number relations.

APPENDIX D

DERIVATION AND JUSTIFICATION

Derivation of Mean Fanning Friction Factor

The mean Fanning friction factor commonly used in fluid mechanics is defined as

$$\bar{f} = - \frac{D}{2\rho\bar{u}^2} \frac{dP}{dx}$$

The classical viscous radial velocity distribution is (ref. 11)

$$u = \frac{1}{2\mu} \frac{dP}{dx} (z^2 - hz)$$

The mean radial velocity is found from

$$\bar{u} = \frac{1}{h} \int_0^h u \, dz = - \frac{h^2}{12\mu} \frac{dP}{dx}$$

or

$$- \frac{dP}{dx} = \frac{12\mu\bar{u}}{h^2}$$

Since $D = 2h$, the mean Fanning friction factor becomes

$$\bar{f} = \frac{24}{Re}$$

Note the Fanning friction factor is one-fourth the Darcy-Weisbach friction factor which is commonly used in hydraulics. (In the text the velocity u is understood to be the mean velocity.)

Validity of Mean Friction Factor Evaluation Using Entrance Reynolds Number

The question arises if it is proper to use the entrance Reynolds number to evaluate the mean friction factor. Examining the Reynolds number,

$$Re = \frac{\rho u 2h}{\mu}$$

or

$$Re = \frac{2\dot{M}}{W\mu} = \frac{constant}{\mu}$$

Hence Re varies inversely with the absolute viscosity of the fluid which in turn varies with the static temperature.

To see the maximum possible change, the maximum temperature possible occurs when $M_1 = 0$ and $M_2 = 1$.

Thus, the exit-entrance temperature ratio can be found using equation (19) and is

$$\frac{T_2}{T_1} = \frac{1 + \frac{\gamma - 1}{2} M_1^2}{1 + \frac{\gamma - 1}{2} M_2^2} = \frac{2}{\gamma + 1}$$

For $\gamma = 1.4$, $T_2/T_1 = 5/6$. This represents about a 17 percent variation in the static temperature for the worst case. From Sutherland's law

$$\mu \propto T^{0.76}$$

$$\overline{f} \propto Re^{-1} \propto \mu \propto T^{0.76}$$

Hence, the maximum viscosity change along the seal leakage path will be small, and the entrance conditions can be used satisfactorily to evaluate the mean friction factor.

REFERENCES

1. Parks, A. J.; McKibbin, A. H.; Ng, C. C. W.; and Slayton, R. M.: Development of Mainshaft Seals for Advanced Air Breathing Propulsion Systems. Rep. PWA-3161, Pratt & Whitney Aircraft (NASA CR-72338), Aug. 14, 1967.

2. Shevchenko, Richard P.: Shaft, Bearing and Seal Systems for a Small Engine. Paper 670064, SAE, Jan. 1967.

3. McKibbin, A. H.; and Parks, A. J.: Aircraft Gas Turbine Mainshaft Face Seals-Problems and Promises. Fourth International Conference on Fluid Sealing. Special Publication SP-2, ASLE, 1969, paper FICFS-28.

4. Johnson, R. L.; and Ludwig, L. P.: Shaft Face Seal With Self-Acting Lift Augmentation for Advanced Gas Turbine Engines. Fourth International Conference on Fluid Sealing. Special Publication SP-2, ASLE, 1969, paper FICFS-27.

5. Ludwig, L. P.; Zuk, J.; and Johnson, R. L.: Use of the Computer in Design of Gas Turbine Mainshaft Seals for Operation to 500 ft/sec (122 m/sec). Presented at 26th Annual Meeting of the National Conference on Fluid Power and the 10th Annual Meeting of the Fluid Power Society, Chicago, Ill., Oct. 13-15, 1970.

6. Gross, William A.: Gas Film Lubrication. John Wiley & Sons, Inc., 1962.

7. Carothers, P. R., Jr.: An Experimental Investigation of the Pressure Distribution of Air in Radial Flow in Thin Films Between Parallel Plates. MS. Thesis, U.S. Navial Post Grad. School, Monterey, Calif., 1961.

8. Grinnell, S. K.: Flow of a Compressible Fluid in a Thin Passage. Trans. ASME, vol. 78, no. 4, May 1956, pp. 765-771.

9. Mueller, Heinz K.: Self Aligning Radial Clearance Seals. Third International Conference cn Fluid Sealing, British Hydromechanics Research Assoc., Cambridge, Eng., Apr. 3-5, 1967, paper H6.

10. Mayer, E. (B.S. Nau, trans.): Mechanical Seals. American Elsevier, 1970.

11. Zuk, John; and Smith, Patricia J.: Computer Program for Viscous, Isothermal Compressible Flow Across a Sealing Dam with Small Tilt Angle. NASA TN D-5373, 1969.

12. Zuk, J.; and Smith, P. J.: Quasi-One-Dimensional Compressible Flow Across Face Seals and Narrow Slots. II - Computer Program. NASA TN D-6787, 1972.

13. Zuk, John; and Ludwig, Lawrence P.: Investigation of Isothermal, Compressible Flow Across a Rotating Sealing Dam. I - Analysis. NASA TN D-5344, 1969.

14. Egli, Adolf: The Leakage of Gases Through Narrow Channels. J. Appl. Mech., vol. 4, no. 2, June 1937, pp. A-63 - A-67.

15. Shapiro, Ascher H.: The Dynamics and Thermodynamics of Compressible Fluid Flow. Vol. I. Ronald Press Co., 1953.

16. Fleming, David P.; and Sparrow, E. M.: Flow in the Hydrodynamic Entrance Region of Ducts of Arbitrary Cross Section. J. Heat Transfer, vol. 91, no. 3, Aug. 1969, pp. 345-354.

17. Lundgren, T. S.; Sparrow, E. M.; and Starr, J. B.: Pressure Drop Due to the Entrance Region in Ducts of Arbitrary Cross Section. J. Basic Eng., vol. 86, no. 3, Sept. 1964, pp. 620-626.

18. Deissler, Robert G.: Analysis of Turbulent Heat Transfer and Flow in the Entrance Regions of Smooth Passages. NACA TN 3016, 1953.

19. Povinelli, V. P.; and McKibbin, A. H.: Development of Mainshaft Seals for Advanced Air Breathing Propulsion Systems, Phase II. Rep. PWA-3933, Pratt & Whitney Aircraft (NASA CR-72737), June 23, 1970.

20. Sabersky, Rolf H.; and Acosta, A. J.: Fluid Flow. Macmillan Co., 1964.

```
016 001 C1 U   15 720505 S00903DS
DEPT OF THE AIR FORCE
AF WEAPONS LAB (AFSC)
TECH LIBRARY/WLOL/
ATTN: E LOU BOWMAN, CHIEF
KIRTLAND AFB NM 87117
```

"The aeronautical and space activities of the United States shall be conducted so as to contribute . . . to the expansion of human knowledge of phenomena in the atmosphere and space. The Administration shall provide for the widest practicable and appropriate dissemination of information concerning its activities and the results thereof."

— NATIONAL AERONAUTICS AND SPACE ACT OF 1958

NASA SCIENTIFIC AND TECHNICAL PUBLICATIONS

TECHNICAL REPORTS: Scientific and technical information considered important, complete, and a lasting contribution to existing knowledge.

TECHNICAL NOTES: Information less broad in scope but nevertheless of importance as a contribution to existing knowledge.

TECHNICAL MEMORANDUMS: Information receiving limited distribution because of preliminary data, security classification, or other reasons.

CONTRACTOR REPORTS: Scientific and technical information generated under a NASA contract or grant and considered an important contribution to existing knowledge.

TECHNICAL TRANSLATIONS: Information published in a foreign language considered to merit NASA distribution in English.

SPECIAL PUBLICATIONS: Information derived from or of value to NASA activities. Publications include conference proceedings, monographs, data compilations, handbooks, sourcebooks, and special bibliographies.

TECHNOLOGY UTILIZATION PUBLICATIONS: Information on technology used by NASA that may be of particular interest in commercial and other non-aerospace applications. Publications include Tech Briefs, Technology Utilization Reports and Technology Surveys.

Details on the availability of these publications may be obtained from:

SCIENTIFIC AND TECHNICAL INFORMATION OFFICE

NATIONAL AERONAUTICS AND SPACE ADMINISTRATION
Washington, D.C. 20546